Inter-subcarrier Nonlinear Interference Canceler for Long-Haul Nyquist-WDM Transmission

Abdelkerim Amari, Philippe Ciblat, and Yves Jaouën

***Abstract*—For long-haul Nyquist-WDM superchannel transmission, an Inter-subcarrier Nonlinear and linear Interference Canceler (INIC) is proposed. This approach consists in detecting the adjacent subcarriers, regenerating them thanks to the Volterra series model of optical fiber, and removing them from the subcarrier of interest. Different ways to implement the INIC are described and compared to the well-known techniques such as digital back propagation (DBP) and Volterra based nonlinear equalizer (VNLE) implemented in a subcarrierwise manner. Significant performance gain (on either the Q factor or transmission distance) is observed. In the context of 400Gbps scheme, the transmission distance gain is up to 500km compared to the DBP and VNLE.**

***Index Terms*—optical communication systems, Nyquist-WDM, digital signal processing, nonlinear interference, Volterra series.**

I. Introduction

NEXT generation of long-haul Wavelength Division Multiplexing (WDM) transmission systems is expected to operate at 400Gbps/1Tbps to satisfy the increasing traffic demand in optical core networks. Such high bit rates require the use of multi-level modulations and subcarrier-multiplexing systems. In that context, superchannel approaches based on Nyquist-WDM [1] and multi-band Orthogonal Frequency Division Multiplexing (MB-OFDM) [2] are the potential candidates in order to reduce the band guard interval. However the use of high spectral efficiency modulation formats such as 16QAM requires higher optical signal-to-noise ratio (OSNR) and so high input powers. Such input powers give rise to nonlinear impairments through the fiber transmission which significantly degrades the system performance. To compensate for these nonlinear impairments, Digital Back Propagation (DBP) via its split-step Fourier implementation [3] and Volterra based-NonLinear Equalizer (VNLE) [4], [5] have been already proposed. However, the performance still degrade rapidly in the context of the superchannel transmission with narrow (up to null) band guard interval. Indeed, the inter-subcarrier nonlinear interference, in addition to the linear cross-band interference, becomes overriding and leads to poor performance.

To deal with the inter-subcarrier interference mitigation, only a few works have been proposed: the cross-phase modulation (XPM) mitigation adapted to DBP [6], the multi-stage successive linear interference cancellation [7], and the tracking equalization due to the equivalent time-varying intersymbol interference model [8]. In [9], we have introduced the Inter-subcarrier Nonlinear and linear Interference Canceler (INIC) and applied it successfully for MB-OFDM. This INIC manages the linear interference due to potential overlapping subcarriers and the so-called Inter-Band Interference. The INIC is then applied to the superchannel Nyquist-WDM context [11]. The Q factor and transmission distance are simulated with respect to the subcarrier spacing and the roll-off for 400Gbps transmission. The proposed INIC outperforms the DBP and VNLE, which were performed individually for each subcarrier.

The paper is organized as follows: in Section II, we introduce the system model. In Section III, the novel INIC receiver is proposed. In Section IV, we provide the simulation results. In Section V, a complexity analysis of the INIC receiver is done. In Section VI, concluding remarks are drawn.

A. Amari, P. Ciblat and Y. Jaouën are with Telecom ParisTech, Université Paris-Saclay, France, email: firstname.name@telecom-paristech.fr

II. System model

We consider an uncompensated standard single mode fiber (SSMF) with N spans, each of length L. The attenuation coefficient, the second-order dispersion parameter, and the nonlinear coefficient are denoted by α, β_2, and γ respectively. Like [12], the Volterra series expansion exhibits an approximate solution of the nonlinear Schrödinger equation that governs the wave propagation within a SSMF. Let $\mathbf{U}$ and $\mathbf{V}$ be the transmit signal in the first span of the fiber and the received signal at the N-th span of the fiber respectively. Due to dual polarization, we denote the components of the signal $\mathbf{U}$ on polarization x and y by U_x and U_y respectively. Moreover, as we consider multi-subcarrier transmission, the transmitted signal can be written (in the frequency domain) by

$$U_{x/y}(\omega) = \sum_{m=1}^{M} U_{x/y,m}(\omega) \tag{1}$$

where $U_{x/y,m}$ is the transmitted signal on the subcarrier m and M is the number of subcarriers. Notice that the transmitted signal $U_{x/y,m}$ is linearly modulated with a sequence of independent information symbols $S_{x/y,m}$. The above model corresponds to the so-called superchannel Nyquist-WDM scheme.

Based on Volterra series expansion model of the optical fiber [12], [5] with equal span, the received signal $V_{x/y}$ on polarization x or y takes the following form

$$\begin{aligned} V_{x/y}(\omega) &= H_1(\omega)U_{x/y}(\omega) \\ &+ \iint H_3(\omega_1,\omega_2,\omega-\omega_1+\omega_2)U_{x/y}(\omega-\omega_1+\omega_2) \\ &\times [U_x(\omega_1)U_x^*(\omega_2)+U_y(\omega_1)U_y^*(\omega_2)]d\omega_1 d\omega_2 \end{aligned} \tag{2}$$

where $()^*$ stands for the complex conjugate, and H_1 and H_3 denote the first-order and third-order Volterra series kernels

respectively. These kernels are given by

$$H_1(\omega) = e^{-j\omega^2\beta_2 NL/2} \quad (3)$$

$$H_3(\omega_1,\omega_2,\omega-\omega_1+\omega_2) = \frac{-jC}{(2\pi)^2}H_1(\omega)\sum_{k=0}^{N-1}e^{-jk\beta_2\Delta\Omega L}$$

with $\Delta\Omega = (\omega_1-\omega)(\omega_1-\omega_2)$, $L_{\text{eff}} = (1-e^{-\alpha L})/\alpha$, and $C = 8\gamma L_{\text{eff}}/9$ [5]. Notice that the Polarization Mode Dispersion (PMD) is not considered in previous equations, but is hereafter simulated and mitigated via the so-called adaptive CMA [10], while the DBP, VNLE and INIC will treat the Chromatic Dispersion (CD) and nonlinear effects jointly. The system (with $M = 4$) is summarized in Fig. 1.

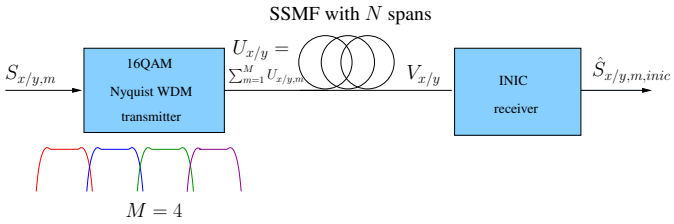

Fig. 1: System model

III. Proposed INIC approach

The main idea of the proposed INIC approach relies on the Decision Feedback Equalizer (DFE) principle [13]. When focusing on one subcarrier of interest (let say m_0); our DFE principle consists in detecting the adjacent subcarriers ($m = m_0+1, m_0-1$), regenerating them, and finally removing them from the subcarrier of interest. The receiver structure is described in Fig. 2 and explained more precisely further.

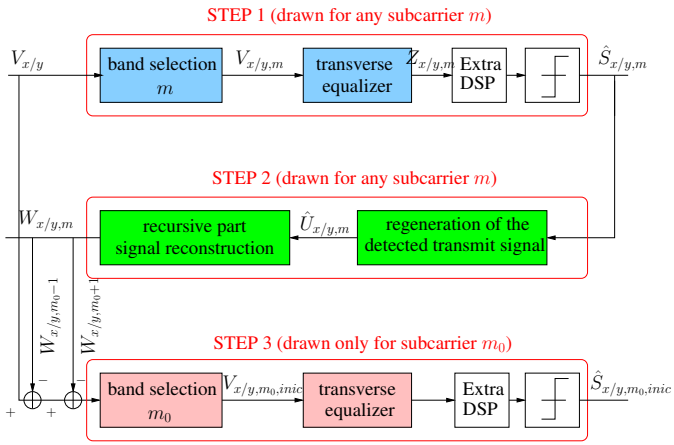

Fig. 2: INIC receiver structure

According to Fig. 2, the INIC structure has two main degrees of freedom: the transverse/feedforward part and the recursive/feedback part. The transverse part is the equalizer (typically the choice can reduce to the order of the Inverse Volterra series). The recursive part corresponds to the way the fiber signal is regenerated (typically the choice can reduce once again to the order of the Volterra series modeling the fiber). In this paper, we implement three INIC receivers: the proposed solution INIC(3,3), the already-existing one INIC(1,1) only adapted to CD linear impairments, and an intermediate one INIC(3,1) where the notation INIC(p,q) stands for a transerve part of order p and a recursive part of order q. Notice that the transverse part deals with the intra-subcarrier compensation whereas the recursive part deals with the inter-subcarrier compensation. In extra DSP block, we handle the PMD thanks to an adaptive CMA and also the phase synchronization thanks to a fourth-power algorithm applied on each subcarrier. For the sake of simplicity, carrier and clock frequency offsets are omitted. Estimators of these offsets can be added in the extra DSP block in order to be robust to these mismatchs.

a) Nonlinear equalizer with nonlinear feedback INIC(3,3): In INIC(3,3), we use the third-order VNLE for the transverse part and the third-order Volterra fiber model for the recursive one. We hereafter assume that the subcarrier of interest is m_0. The other subcarriers can be treated in a similar way. The implementation of the INIC(3,3) for the subcarrier m_0 can be split into three steps:

In the first step, each subcarrier is selected through a band-pass filter, leading to $V_{x/y,m}$, and then demodulated according to the third-order VNLE. The output of the VNLE is denoted by $Z_{x/y,m}$ and writes as

$$\begin{aligned} Z_{x/y,m}(\omega) &= K_1(\omega)V_{x/y,m}(\omega) \\ &+ \iint K_3(\omega_1,\omega_2,\omega-\omega_1+\omega_2)V_{x/y,m}(\omega-\omega_1+\omega_2) \\ &\times [V_{x,m}(\omega_1)V^*_{x,m}(\omega_2)+V_{y,m}(\omega_1)V^*_{y,m}(\omega_2)]d\omega_1 d\omega_2 \end{aligned} \quad (4)$$

where K_1 and K_3 are the first-order and third-order inverse Volterra kernels respectively [5]. Then, a threshold detector is applied on $Z_{x/y,m}$ for each subcarrier m in order to find out the detected symbols $\widehat{S}_{x/y,m}$ related to $S_{x/y,m}$.

In the second step, the detected symbols of each interference subcarrier m are re-modulated and regenerated based on third order Volterra model of the optical fiber. Thus, the output $W_{x/y,m}$ can be written as:

$$\begin{aligned} W_{x/y,m}(\omega) &= H_1(\omega)\widehat{U}_{x/y,m}(\omega) \\ &+ \iint H_3(\omega_1,\omega_2,\omega-\omega_1+\omega_2)\widehat{U}_{x/y,m}(\omega-\omega_1+\omega_2) \\ &\times [\widehat{U}_{x,m}(\omega_1)\widehat{U}^*_{x,m}(\omega_2)+\widehat{U}_{y,m}(\omega_1)\widehat{U}^*_{y,m}(\omega_2)]d\omega_1 d\omega_2 \end{aligned} \quad (5)$$

where $\widehat{\mathbf{U}} = [\widehat{U}_{x,m}, \widehat{U}_{y,m}]$ is the re-modulated signal corresponding to the detected symbols $\widehat{\mathbf{S}} = [\widehat{S}_{x,m}, \widehat{S}_{y,m}]$. Because of the bandwidth overlap (either non-null roll-off or super-Nyquist) and the nonlinear effects, the signal $W_{x,m}$ is not only on subcarrier m but also spreads over the adjacent subcarriers. In practice, the interference is mainly spread over the two closest adjacent subcarriers.

In the third step, the two closest adjacent subcarriers signals $\mathbf{W}_{m_0-1}$ and $\mathbf{W}_{m_0+1}$ are subtracted from the original received signal $\mathbf{V}$ in order to obtain

$$\mathbf{V}_{m_0,inic}(\omega) = \mathbf{V}(\omega) - \mathbf{W}_{m_0-1}(\omega) - \mathbf{W}_{m_0+1}(\omega). \quad (6)$$

The final decision $\widehat{\mathbf{S}}_{m_0,inic}$ is made on the signal $\mathbf{V}_{m_0,inic}$ after it has been passed through the subcarrier selection m_0 as well as through the VNLE to compensate for the intra-subcarrier nonlinear effects.

b) Nonlinear equalizer with linear feedback INIC(3,1): In INIC(3,1), the third-order VNLE is used for the intra-subcarrier nonlinearities compensation but only linear interference (due to bandwidth overlapping) with adjacent subcarriers is considered. Therefore the recursive part relies on the first-order Volterra optical fiber model. Thus, Eq. (5) becomes

$$W_{x/y,m}(\omega) = H_1(\omega)\widehat{U}_{x/y,m}(\omega). \tag{7}$$

As in Eq. (6), before taking the final decision, $\mathbf{V}_{m_0,inic}$ is passed through the third-order VNLE to mitigate the intra-subcarrier nonlinear effects.

c) Linear equalizer with linear feedback INIC(1,1): In INIC(1,1), already proposed by [7], the nonlinear effects are not taken into account and the receiver only mitigates the intra-subcarrier and inter-subcarrier linear effects. INIC(1,1) represents the State-of-the-Art. More precisely, the received signal $V_{x/y,m}$ is linearly equalized and $Z_{x/y,m}$ is given by

$$Z_{x/y,m}(\omega) = K_1(\omega)V_{x/y,m}(\omega). \tag{8}$$

After detection on $Z_{x/y,m}$ to get $\widehat{S}_{x/y,m}$, the re-modulated signal $\widehat{U}_{x/y,m}$ goes to the first-order Volterra model and the output $W_{x/y,m}$ is given by Eq. (7). We then apply Eq. (6), and the obtained signal $\mathbf{V}_{m_0,inic}$ goes through the linear equalizer.

IV. Simulation Results

We evaluate the performance of the proposed INIC by simulation. We generate a dual-polarization 16QAM modulated Nyquist-WDM superchannel with 4 subcarriers. The bit rate is 448Gbps and the symbol rate per subcarrier and per polarization is $R = 14$GBaud. The transmission line consists of multi-span SSMF with $\alpha = 0.2\text{dB.km}^{-1}$, $D = 17\text{ps.nm}^{-1}\text{.km}^{-1}$ with $D = 2\pi c\beta_2/\lambda^2$ and $\lambda = 1550$nm, and $\gamma = 1.4\text{W}^{-1}\text{.km}^{-1}$. The PMD is $0.1\text{ps.km}^{-1/2}$. The shaping filter is a Root-Raised Cosine (RRC) with roll-off ρ. An Erbium-Doped Fiber Amplifier (EDFA) with a 5.5dB noise figure and a 20dB gain is used at each span of 100km. Notice that the analog to digital converter (ADC) works at twice the symbol rate. Polarization arrangement and phase compensation are done as explained in Section III. Table I summarizes the simulation parameters. All results will concern the central subcarriers. The input power corresponds to those consumed on the whole bandwith and both polarizations, i.e., by one WDM wavelength. We also define the subcarrier spacing factor

TABLE I: Simulation parameters

Subcarrier number M	4
Bit rate	448Gbps
Symbol rate R	14GBd
Modulation	16QAM
RRC roll-off ρ	0.1 or 0.01
Subcarrier spacing factor δ	from 0.9 to 1.1
Samples per symbol	2
EDFA noise figure	5.5dB
Span length L	100km

δ as the ratio between the subcarrier spacing Δf and the symbol rate R, i.e., $\delta = \Delta f/R$.

In any figure, we plot the performance of each INIC receiver, and for comparison the (8-step per span) DBP, the standard third-order VNLE, and the linear equalizer. Unless otherwise stated, the transmission distance is $d = 1000$km.

We fix the roll-off ρ to be 0.1. In Fig. 3, we plot the Q factor versus the input power per subcarrier for a subcarrier spacing factor $\delta = 1$. We observe that DBP, VNLE and linear equalizer offers similar performance far away from those proposed by the INIC. So the inter-subcarrier interference strongly disturbs the performance and has to be mitigated. The INIC(3,3) is the best ones and offers a gain about 0.3dB, 0.6dB and 1.5dB with respect to the INIC(3,1), the INIC(1,1) and the DBP.

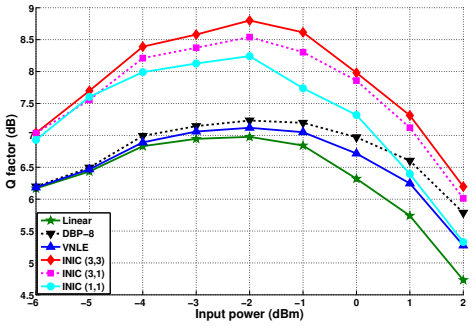

Fig. 3: Q factor vs. input power ($\rho = 0.1$, $\delta = 1$)

In Fig. 4, we plot the Q factor versus the subcarrier spacing factor δ at the optimum input power. When super-Nyquist WDM is considered (i.e., $\delta < 1$), the performance of DBP and VNLE are strongly reduced because of the high linear and nonlinear inter-subcarrier interference. At $\delta = 0.95$, INIC(3,3) offers a gain of 2dB in comparison with DBP and VNLE and 0.5dB in comparison with INIC(3,1). At $\delta = 1.1$, INIC(3,1) and INIC(3,3) leads to the same performance as DBP and VNLE due to the absence of subcarrier interference while INIC(1,1) is close to the linear receiver since the intra-channel nonlinear interference is not treated and the inter-channel interference is negligible.

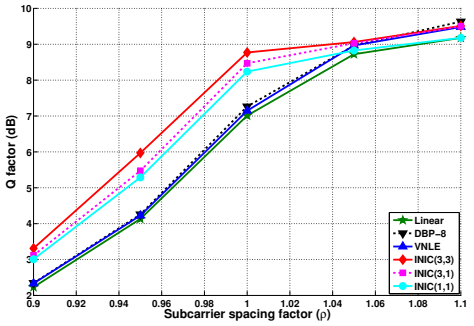

Fig. 4: Q factor vs. subcarrier spacing factor δ ($\rho = 0.1$)

In Fig. 5, we plot the transmission reach versus the input power per subcarrier for the Soft Decision Forward Error Correction limit $Q = 5.9$dB. INIC(3,3) improves the transmission reach by 500km compared to DBP, VNLE and linear INIC(1,1). Similar performance are obtained for INIC(3,3) and INIC(3,1) and the gain is less than the span length.

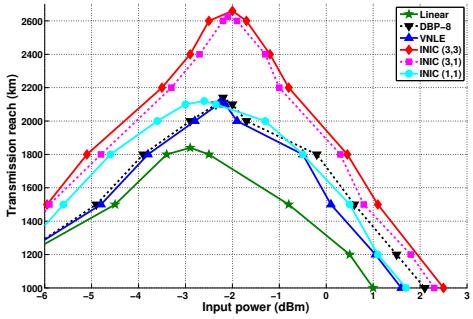

Fig. 5: Transmission reach vs. input power ($\rho = 0.1$, $\delta = 1$)

We now fix the roll-off ρ to be 0.01. In Fig. 6, we plot the Q factor versus the input power per subcarrier for a subcarrier spacing factor $\delta = 0.95$. INIC (3,3) still outperforms INIC(3,1), INIC(1,1) and DBP with 0.5dB, 0.7dB and 1.8dB of gain respectively. This substantial gain is due to the non-negligible inter-subcarrier nonlinear interference at $\delta = 0.95$.

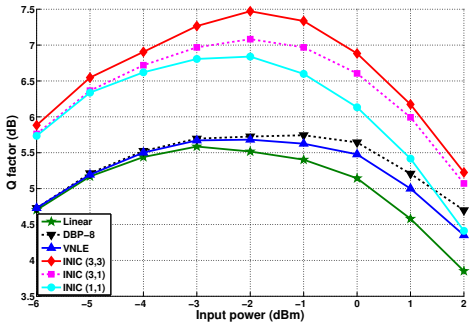

Fig. 6: Q factor vs. input power ($\rho = 0.01$, $\delta = 0.95$)

In Fig. 7, we plot the Q factor versus the subcarrier spacing factor δ at optimum input power. The INIC receiver gain reduces dramatically as soon as $\delta \geq 1$ (the subcarrier interference becomes very weak) and $\delta \leq 0.9$ (the interference is too high and hard to compensate for due to the numerous errors in the first step of the INIC).

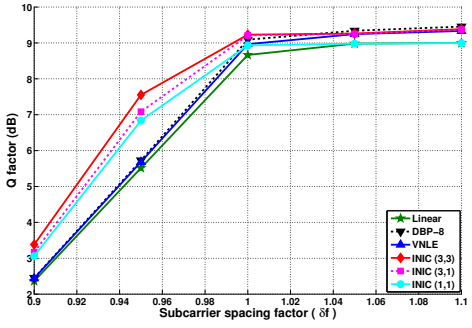

Fig. 7: Q factor vs. subcarrier spacing factor δ ($\rho = 0.01$)

V. Complexity Analysis

The complexity is very roughly analyzed through the required number of real multiplications. According to [5], the complexity of the single-step DBP and the third-order VLNE per subcarrier are $C_{\text{single-step DBP}} = 4NN_f \log_2(N_f) + 10.5NN_f$ and $C_{\text{VLNE}} = 2NN_f \log_2(N_f) + 4.25NN_f$ respectively, where N_f is the size of the implemented FFT. So $C_{\text{single-step DBP}} \approx 2C_{\text{VLNE}}$. Complexity of applying H_1 and H_3 is almost equal to that of K_1 and K_3, we have $C_{\text{INIC(3,3)}} = 3C_{\text{VLNE}} = (3/2)C_{\text{single-step DBP}}$ because we need to regenerate the two adjacent subcarriers and to pass them through the VNLE. Notice that the VNLEs applied on $m_0 - 1$ and $m_0 + 1$ in the first step are not considered since they are done even in absence of INIC, just for decoding these subcarriers. As for INIC(3,1), the recursive part is linear and needs $4N_f \log_2(N_f) + 4N_f$ real multiplications. If N is large enough, this term can be neglected and we so have $C_{\text{INIC(3,1)}} = 2C_{\text{VLNE}} = C_{\text{single-step DBP}}$. Consequently, INIC(3,3) and INIC(3,1) are much less complex than the eight-step per span DBP used in simulation. We have neglected the complexity of the extra DSP since CMA and Viterbi-Viterbi algorithm are necessary done in step 1 whatever the receiver, and so the only extra complexity lies in step 3 which can be well initialized with the output of the step 1.

VI. Conclusion

New methods for the inter-subcarrier nonlinear interference mitigation have been proposed for the long-haul superchannel Nyquist-WDM context. They significantly improve the Q factor compared to DBP and VNLE in the presence of spectral overlap. As a future work, INIC can rely on other nonlinear compensation technique such as DBP. This Decision-Feedback approach can be also used for combating the intra-subcarrier nonlinear effect as partially treated in [14].

References

[1] J. Renaudier et al., "Spectrally efficient 1Tb/s Transceivers," OFC, M2G.3, 2015.

[2] S. Chandrasekhar, "OFDM based superchannel transmission technology," J. Lightwave Technol., vol.**30**, pp.3816-3823, 2012.

[3] E. Ip et al., "Compensation of dispersion and nonlinear impairments using digital back propagation," J. Lightwave Technol., vol.**26**, no.20, pp.3416-3425, 2008.

[4] J. D. Reis et al., "Unveiling nonlinear effects in dense coherent optical WDM systems with Volterra series," Opt. Expr., vol.**18**, no.8, pp.8660-8670, 2010.

[5] L. Lui et al., "Intrachannel Nonlinearity Compensation by Inverse Volterra Series Transfer Function," J. Lightwave Technol., vol.**30**, no.3, pp.310-316, 2012.

[6] F. Zhang et al., "XPM Model Based Digital Backpropagation for Subcarrier-Multiplexing Systems," J. Lightwave Technol., vol.**33**, no.24, pp.5140-5150, 2015.

[7] K. Shibahara et al.,"Multi-stage successive interference cancellation for spectrally-efficient super-Nyquist transmission," ECOC, Th1.6.4, 2015.

[8] R. Dar et al., "Inter-channel nonlinear interference noise in WDM systems: modeling and mitigation," J. Lightwave Technol., vol.**33**, no.5, pp.1044-1053, 2015.

[9] A. Amari et al.,"Inter-Band Nonlinear Interference Canceler for Long-Haul coherent optical OFDM Transmission," TIWDC, pp.17-19, 2015.

[10] S. Savory, "Digital filters for coherent optical receivers," Opt. Expr., vol.**16**, no.2, pp.804-817, 2008.

[11] J. Yu et al., "Transmission of 8 480-Gb/s super-Nyquist-filtering 9-QAM-like signal at 100 GHz-grid over 5000-km SMF-28 and twenty-five 100 GHz-grid ROADMs," Opt. Expr., vol.**21**, pp.15686-15691, 2013.

[12] K. Peddanarappagari et al., "Volterra series transfer function of single-mode fibers," J. Lightwave Technol., vol.**15**, no.12, pp.2232-2241, 1997.

[13] D. D. Falconer, "Adaptive equalization of channel nonlinearities in QAM data transmission systems," Bell System Technical J., vol.**57**, no.7, 1978.

[14] D. Maiti et al., "Modified Nonlinear Decision Feedback Equalizer for Long-Haul Fiber-Optic Communications," J. Lightwave Technol., vol.**33**, no.18, pp.3763-3772, 2015.